

# On Generating Explanations for Reinforcement Learning Policies: An Empirical Study

Mikihisa Yuasa<sup>1</sup>, Huy T. Tran<sup>1</sup>, and Ramavarapu S. Sreenivas<sup>2</sup>

**Abstract**—Understanding a *reinforcement learning* policy, which guides state-to-action mappings to maximize rewards, necessitates an accompanying explanation for human comprehension. In this paper, we introduce a set of *linear temporal logic* (LTL) formulae designed to provide explanations for policies, and an algorithm for searching through those formulae for the one that best explains a given policy. Our focus is on crafting explanations that elucidate both the ultimate objectives accomplished by the policy and the prerequisite conditions it upholds throughout its execution. These LTL-based explanations feature a structured representation, which is particularly well-suited for local-search techniques. The effectiveness of our proposed approach is illustrated through a simulated game of capture the flag and a car-parking environment. The paper concludes with suggested directions for future research.

## I. INTRODUCTION

*Reinforcement learning* (RL) stands as a formidable subfield within machine learning, experiencing an extraordinary surge in both acclaim and accomplishments in recent times. It has ushered in a transformative era across various domains by virtue of its capacity to autonomously acquire knowledge and formulate decisions within intricate environments. Whether it is triumphing over world champions in games such as Chess and Go or enhancing recommendation systems and robotics, RL has unmistakably demonstrated its vast potential [1]–[3].

The adoption of deep learning techniques in RL, commonly referred to as *deep reinforcement learning* (DRL), has further propelled the field, enabling agents to achieve remarkable feats that were once thought to be beyond the realm of possibility [4], [5]. However, this increasing complexity and depth in RL models has also given rise to a pressing concern: their explainability and interpretability [6], [7]. As DRL systems evolve to tackle real-world problems, their decision-making processes become increasingly opaque, making it challenging to understand why they make certain choices.

A common approach to explaining complex policies, such as those produced by DRL, is to mine *temporal logic* specifications from observed system behaviors and environment interactions [8]. Temporal logic provides formalism and semantics to describe temporal development of system states in a human-interpretable manner [8], [9]. These works use a variety of techniques, such as directed acyclic graphs, boosted decision trees, and neural networks for different applications and assumptions [8]. They are mainly template-based; namely, they assume the structure

of temporal logic specification to be mined from policies, actions, or trajectories [8], [10]–[13]. However, to our best knowledge, these templates do not support conjunctions or disjunctions within temporal clauses. For example, [10] can only infer set combinations of temporal clauses, and [13] neither supports conjunctions nor disjunctions within an “eventually” clause. In this work, we focus on a template which allows conjunctions and disjunctions within temporal clauses, which is useful for task and safety specifications for robotics applications. Furthermore, our approach does not require the search process and policy optimization process to happen simultaneously, which can contribute to faster exploration of search hyperparameters.

We propose an algorithm for generating a cogent explanation for a given target RL policy, where this explanation delineates both the operational conditions maintained throughout execution, as well as the ultimate objectives achieved by the policy. Our approach centers on a family of *linear temporal logic* (LTL) formulae that is endowed with a concept of neighborhood, which in turn is amenable to a local-search algorithm (see Section III). In our method, each potential LTL-explanation is effectively translated into an RL policy using established techniques in the literature [9]. We then gauge the alignment of this representative policy with the target policy by employing a well-structured metric (see Section III-B). Should a neighboring LTL-explanation exhibit superior alignment with the target policy according to this metric, it supplants the current explanation. This iterative process persists until none of the neighboring LTL-explanations surpasses the present one, thus establishing a local optimum as the recommended LTL-explanation. To enhance robustness, we propose additional neighborhood expansion and extension heuristics, as well as a multi-start implementation of the search that generates the top- $k$  (e.g.,  $k = 10$ ) LTL specifications as candidate explanations. Our method is essentially a type of inverse reinforcement learning (IRL) [14] that approximates the target policy as an RL policy optimized for an LTL reward.

In short, our contributions are: (1) we propose a novel local-search method to find a formal LTL specification that best-explains an RL policy, and (2) we demonstrate our method on two simulated robotics applications (a game of capture the flag and a car-parking environment).

The rest of the paper is organized as follows: Section II presents a review of relevant background material, which is followed by a detailed treatment of our search procedure in Section III. Section IV presents the results of our validation experiments. The paper concludes with a summary and

<sup>1</sup>Aerospace Engineering, University of Illinois at Urbana-Champaign, Urbana, IL 61801 USA. {myuasa2, huytran1}@illinois.edu

<sup>2</sup>Industrial and Enterprise Systems Engineering, University of Illinois at Urbana-Champaign, Urbana, IL 61801 USA. rsree@illinois.edu

suggestions for future research in Section V.

## II. BACKGROUND

### A. Reinforcement Learning

We model our problem as a *Markov decision process* (MDP)  $\mathcal{M}$  defined by a tuple  $(\mathcal{S}, \mathcal{A}, p, r, \gamma)$  [15], where  $\mathcal{S}$  is the state space,  $\mathcal{A}$  is the action space of the agent, and  $\gamma \in [0, 1)$  is the discount factor. Then  $p(s'|s, a) : \mathcal{S} \times \mathcal{A} \times \mathcal{S} \mapsto [0, 1]$  is the state transition function and  $r(s, a, s') : \mathcal{S} \times \mathcal{A} \times \mathcal{S} \mapsto \mathbb{R}$  is the reward function for states  $s, s' \in \mathcal{S}$  and action  $a \in \mathcal{A}$ . At time step  $t$ , the agent executes an action  $a_t$  given the current state  $s_t$ , after which the system transitions to state  $s_{t+1}$  and the agent receives reward  $r(s_t, a_t, s_{t+1})$ . Let  $\pi(a|s) : \mathcal{S} \times \mathcal{A} \mapsto [0, 1]$  be a policy for the agent. The objective in RL is to learn a policy that maximizes the expected sum of discounted rewards  $\mathbb{E}_{p, \pi} \{ \sum_{t=0}^{\infty} \gamma^t r(s_t, a_t, s_{t+1}) \mid s_0 = s, a_0 = a \}$  [16], [17].

### B. Linear Temporal Logic

Using Backus-Naur form, the syntax for LTL is defined as  $\phi := \top \mid f(s) < c \mid \neg\phi \mid \phi \vee \psi \mid \phi \wedge \psi \mid \mathcal{G}(\phi) \mid \mathcal{F}(\phi) \mid \mathcal{U}(\phi) \mid \mathcal{X}(\phi)$  for logical formulae  $\phi$  and  $\psi$ . Here,  $\top$  is the True Boolean constant,  $s \in \mathcal{S}$  is an MDP state,  $f(s) < c$  is a predicate over  $s$  for  $c \in \mathbb{R}$ , and  $\neg$  (negation),  $\wedge$  (conjunction), and  $\vee$  (disjunction) are Boolean connectives.  $\mathcal{F}$  (eventually),  $\mathcal{G}$  (globally),  $\mathcal{U}$  (until), and  $\mathcal{X}$  (next) are temporal operators. We restrict attention to propositions that are expressed in their *Conjunctive Normal Form* (CNF) or *Disjunctive Normal Form* (DNF), and we require that each temporal clause can have up to two clauses within it.

A feasible LTL-specification can be transformed into a *Finite State Predicate Automaton* (FSPA) using  $\omega$ -automaton manipulation with the help of model checking packages such as Spot [9], [18], [19]. A transition between automaton edges is described as a logical formula, and only one transition, including one that loops back to the current edge, is possible for a time step [20]. More formally, an FSPA  $\mathcal{A}$  is defined by a tuple  $(\mathcal{Q}, \mathcal{S}, \mathcal{E}, \Psi, q_0, b, F, Tr)$ . Here,  $\mathcal{Q}$  is a finite set of automaton states,  $\mathcal{S}$  is an MDP state space,  $\mathcal{E} \subseteq \mathcal{Q} \times \mathcal{Q}$  is the set of edges (transitions) between automaton states,  $\Psi$  is the set of input atomic predicates,  $q_0 \in \mathcal{Q}$  is the initial automaton state,  $b : \mathcal{E} \mapsto \Psi$  maps the edges  $\mathcal{E}$  to predicate Boolean formulae composed by  $\Psi$ ,  $F \subseteq \mathcal{Q}$  is the set of final (accepting) automaton states, and  $Tr$  is the set of trap states. When presented with an LTL formula and a sequence of states within the FSPA, we can assign a real-number value, the robustness, that reflects the degree to which the LTL formula is satisfied by the given state sequence. In this context, a higher robustness value signifies a more substantial level of satisfaction. Given a state  $s \in \mathcal{S}$  and logical formulae  $\phi, \psi$ , the robustness is defined as,

$$\begin{aligned} \rho(s, f(s) < c) &= c - f(s), \\ \rho(s, \neg\phi) &= -\rho(s, \phi), \\ \rho(s, \phi \wedge \psi) &= \min(\rho(s, \phi), \rho(s, \psi)), \\ \rho(s, \phi \vee \psi) &= \max(\rho(s, \phi), \rho(s, \psi)), \end{aligned}$$

where  $c \in \mathbb{R}$  is a constant value. Given a trajectory of states  $\tau := (s_1, s_2, \dots, s_k)$  where  $k$  is the length of the trajectory, the robustness of temporal operators are defined as,

$$\begin{aligned} \rho(\tau, \mathcal{F}(\phi)) &= \max_{i \in [1, k]} (\rho(s_i, \phi)), \\ \rho(\tau, \mathcal{G}(\phi)) &= \min_{i \in [1, k]} (\rho(s_i, \phi)), \end{aligned}$$

where  $\phi$  is a logical formula.

### C. FSPA-Augmented MDP

We now define an FSPA-augmented MDP  $\mathcal{M}_{\mathcal{A}}$  based on the formulation in [9], [21], [22]. Given MDP  $\mathcal{M}$  and FSPA  $\mathcal{A}$ , an FSPA-augmented MDP  $\mathcal{M}_{\mathcal{A}}$  is defined by a tuple  $(\tilde{\mathcal{S}}, \mathcal{Q}, \mathcal{A}, \tilde{p}, \tilde{r}, \mathcal{E}, \Psi, q_0, b, F, Tr)$ . Here,  $\tilde{\mathcal{S}} \subseteq \mathcal{S} \times \mathcal{Q}$  is the product state space. Then  $\tilde{p}(\tilde{s}'|\tilde{s}, a) : \tilde{\mathcal{S}} \times \mathcal{A} \times \tilde{\mathcal{S}} \mapsto [0, 1]$  is the state transition function and  $\tilde{r}(\tilde{s}, a, \tilde{s}') : \tilde{\mathcal{S}} \times \mathcal{A} \times \tilde{\mathcal{S}} \mapsto \mathbb{R}$  is the reward function for states  $\tilde{s}, \tilde{s}' \in \tilde{\mathcal{S}}$  and action  $a \in \mathcal{A}$ . The reward  $\tilde{r}$  is defined for sparse rewards as,

$$\tilde{r}(\tilde{s}, a, \tilde{s}') = \begin{cases} 0 & q = q', \\ -\rho(s, b(q, q')) & q' \in Tr, \\ \rho(s, b(q, q')) & \text{otherwise,} \end{cases} \quad (1)$$

where  $\rho(s, b(q, q'))$  is the transition robustness for  $s \in \mathcal{S}$  and  $q, q' \in \mathcal{Q}$ . For dense rewards, when  $q = q'$ , the reward is defined as  $\tilde{r}(\tilde{s}, a, \tilde{s}') = \beta \rho(s, b(q, q'))$  given a scaling factor  $\beta \in \mathbb{R}$  and  $q'' \in \mathcal{Q} \setminus Tr$  s.t.  $q'' \neq q$ . The intuition of this dense reward is that, if the next automaton state is the same as the current automaton state, the reward encourages a transition to a non-trap automaton state.

## III. METHOD

We propose a heuristic tree search algorithm that aims to find a human-readable explanation of an arbitrary target policy whose action distribution is accessible. Each node in our search represents a possible explanation in the form of an LTL specification, composed from a user-specified set of atomic predicates. Figure 1 illustrates the high-level architecture of the algorithm, with Algorithms 1 and 2 providing more detailed pseudo-code. We detail the key components of our algorithm below.

### A. Node Definition

We use two, out of four, temporal operators to explain policies: the global-operator  $\mathcal{G}(\bullet)$  indicates that the propositional argument must hold throughout all future time steps; the eventually-operator  $\mathcal{F}(\bullet)$  specifies that the propositional argument must hold at some point in the future. Using these operators, we consider the class of LTL-specifications of the form  $\mathcal{F}(\bullet) \wedge \mathcal{G}(\bullet)$ . We choose this form because our primary focus is on robotics applications, where we assume a robot tries to achieve certain tasks expressed in  $\mathcal{F}(\bullet)$  while satisfying global safety constraints expressed in  $\mathcal{G}(\bullet)$ . For example, given a set of atomic predicates  $\Phi := \{\psi_1, \psi_2, \psi_3, \psi_4, \psi_5\}$ , a possible specification is  $\mathcal{F}(\psi_1 \vee \psi_2) \wedge \mathcal{G}(\neg\psi_3 \wedge (\neg\psi_4 \vee \psi_5))$ . In plain English, this specification requires that: “*Eventually, either  $\psi_1$  or  $\psi_2$  is satisfied. Globally,  $\psi_3$  is not satisfied and either  $\psi_4$  is not satisfied or  $\psi_5$  is satisfied*”. As noted in

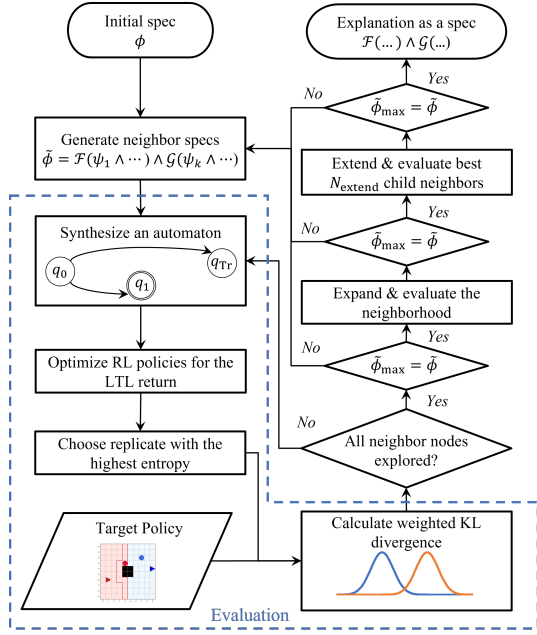


Fig. 1. Overview of our proposed search algorithm.

TABLE I  
THE TABULAR REPRESENTATION OF SPECIFICATION

$$\mathcal{F}(\psi_1 \vee \psi_2) \wedge \mathcal{G}(\neg\psi_3 \wedge (\neg\psi_4 \vee \psi_5))$$

	$\psi_1$	$\psi_2$	$\psi_3$	$\psi_4$	$\psi_5$	$\mathcal{F}(\bullet)$	$\mathcal{G}(\bullet)$
$\psi_i / \neg\psi_i$	0	0	1	1	0	-	-
$\mathcal{F}/\mathcal{G}$	0	0	1	1	1	-	-
Clause 0 / 1	0	0	0	1	1	-	-
CNF / DNF	-	-	-	-	-	1	0

Section III-C, this collection of LTL-formulae is strongly-connected through a series of unitary operations. This means that any LTL-formula within this set can be converted into another through a (short) sequence of unitary syntax modifications. The selection of atomic predicates is application-dependent and continues to stand as a pivotal design decision.

Each node in our search is defined as a row vector of truth values whose length is  $3N_{\text{pred}} + 2$ , where  $N_{\text{pred}}$  is the number of atomic predicates. The first  $N_{\text{pred}}$  elements of the vector define whether or not each predicate is negated (0 for no negation, 1 for negation). The next  $N_{\text{pred}}$  elements define which temporal formula,  $\mathcal{F}(\bullet)$  or  $\mathcal{G}(\bullet)$ , each predicate belongs to (0 for  $\mathcal{F}$ , 1 for  $\mathcal{G}$ ). We require each temporal formula to contain at least one predicate. The following  $N_{\text{pred}}$  elements define which clause within the temporal formula each predicate belongs to (0 for the first clause, 1 for the second clause). We allow up to two clauses within each temporal formula for this paper, but note that the number of such clauses is arbitrary. The last two elements define whether each temporal formula,  $\mathcal{F}(\bullet)$  or  $\mathcal{G}(\bullet)$ , is in CNF or DNF form (0 for CNF, 1 for DNF). Table I shows the row vector representation, in tabular form, for the previously mentioned example specification.

## B. Node Evaluation

We evaluate the utility of a node as a possible explanation by measuring the similarity between a policy optimized for that node’s specification and the target policy. More specifically, we first synthesize the FSPA  $\mathcal{A}$  associated with a node’s specification  $\phi$ , and construct the resulting FSPA-augmented MDP  $\mathcal{M}_{\mathcal{A}}$ . We then use RL to optimize a policy with respect to the augmented reward  $\tilde{r}$ . We address the fact that multiple optimal policies can exist for a given MDP [23] by optimizing  $N_{\text{rep}}$  replicates for a given node and choosing the policy with the highest policy entropy to represent that node. We estimate each policy’s entropy using,

$$\bar{H}(\pi, s, \mathcal{B}_{\text{NT}}) = \frac{-\sum_{s \in \mathcal{B}_{\text{NT}}} \pi(\cdot|s) \log \pi(\cdot|s)}{|\mathcal{B}_{\text{NT}}|}, \quad (2)$$

where  $\mathcal{B}_{\text{NT}}$  is a set of randomly sampled non-trap states. Here, a non-trap state is a state  $s \in \mathcal{S}$  such that  $\rho(s, b(q, q')) > 0 \iff q, q' \in \mathcal{Q} \setminus \text{Tr}$ .

We then measure the similarity between the selected policy and the target policy by calculating KL divergence values over action distributions of sampled states. More specifically, for a selected policy  $\pi_\phi$ , target policy  $\pi_{\text{tar}}$ , and state  $s$ , we calculate,

$$D_{\text{KL}}(A_\phi || A_{\text{tar}}) = A_\phi \log \frac{A_\phi}{A_{\text{tar}}}, \quad (3)$$

where  $A_\phi := \pi_\phi(\cdot|s)$  and  $A_{\text{tar}} := \pi_{\text{tar}}(\cdot|s)$  are the action distributions for the selected policy and target policy, respectively, at state  $s$ . In cases where policies output multiple actions (as in our parking environment), the mean KL divergence value is used, averaged over the action distribution pairs. Finally, we use Equation (3) to calculate the utility of node specification  $\phi$  as a weighted average of KL divergence (*wKL divergence*) values over randomly sampled non-trap states,

$$U(\pi_\phi, \pi_{\text{tar}}, \mathcal{B}_{\text{NT}}) = -\sum_{i=1}^{|\mathcal{B}_{\text{NT}}|} w_i D_{\text{KL}}(\pi_\phi, \pi_{\text{tar}}, s_i), \quad (4)$$

where  $\mathcal{B}_{\text{NT}}$  is a set of randomly sampled non-trap states,  $s_i \in \mathcal{B}_{\text{NT}}$ , and  $w_i$  is the weight associated with  $s_i$ . We define these weights as,

$$w_i := \frac{H(\pi_{\text{tar}}, s_i)}{\sum_{s_j \in \mathcal{B}_{\text{NT}}} H(\pi_{\text{tar}}, s_j)}, \quad (5)$$

where  $H(\pi_{\text{tar}}, s)$  is a normalized entropy calculated as,

$$H(\pi_{\text{tar}}, s) := 1 + \frac{\pi_{\text{tar}}(\cdot|s) \log \pi_{\text{tar}}(\cdot|s)}{H_{\text{max}}}, \quad (6)$$

and  $H_{\text{max}}$  is the maximum possible entropy. We use a weighted average to emphasize similarity between policies at states where the target policy is highly certain about what action to take.

We include an augmented return filter to ignore any nodes that produce a policy with a converged return lower than a user-defined threshold  $\tilde{R}_{\text{fin}}$ . This filter thus ignores specifications that are impossible to satisfy given the FSPA-augmented MDP.

### C. Neighborhood Definition and Evaluation

After evaluating a node specification  $\phi$ , our search proceeds by generating a neighborhood  $\mathcal{N}(\phi)$  of related specifications. We define the neighborhood  $\mathcal{N}(\phi)$  as the set of specifications whose row vector representations differ from that of  $\phi$  at a single location (i.e., a single bit-flip). It is not hard to see that the class of LTL-formulae considered in this paper (i.e., of the form  $\mathcal{F}(\bullet) \wedge \mathcal{G}(\bullet)$ ) are completely connected under this notion of a neighborhood. After generating  $\mathcal{N}(\phi)$ , we evaluate each of the neighboring nodes using the method discussed in Section III-B.

### D. Additional Neighborhood Expansion & Extension

To address the potential existence of multiple undesired local optima, we also include additional neighborhood expansion and extension steps in our search. The expansion step creates an expanded neighborhood  $\mathcal{N}_{\text{exp}}(\phi)$  for a given parent node specification  $\phi$  by flipping the values of the last two elements (i.e., the elements that define whether the temporal formulae are in CNF or DNF form) of each specification in the original neighborhood  $\mathcal{N}(\phi)$ . These additional nodes are then evaluated. This expansion step is implemented if the original neighborhood of  $\phi$  does not produce a better specification than  $\phi$ .

We also include an extension step that forces the search to generate and evaluate neighborhoods for the child nodes in  $\mathcal{N}(\phi)$ , even when the nodes in  $\mathcal{N}(\phi)$  have a lower utility than  $\phi$ . That is, we extend the search by evaluating neighbors of the nodes in  $\mathcal{N}(\phi)$  with the highest utilities, up to  $N_{\text{extend}}$  times. This extension step is implemented if the original and extended neighborhoods of  $\phi$  do not produce a better specification than  $\phi$ .

## IV. RESULTS

### A. Test Environments

We demonstrate our proposed method in two environments: a game of capture the flag (CtF) and a car-parking scenario. The CtF game is a simple grid-world environment (i.e., discrete state and action spaces), but includes complex adversarial dynamics, as shown in Figure 2. The car-parking scenario is used to test our method’s ability to scale to continuous state spaces, as shown in Figure 3. We use RL policies optimized for LTL specifications as target policies for this work, to allow us to easily determine if the true explanation was found by our method. However, our method can be applied to any decision policy, assuming we are given access to its action distribution outputs for observed states.

1) *CtF Game*: In our CtF game, if the two agents are next to each other in the blue territory, then the red agent is killed with 75% probability (and vice versa in the red territory). The game ends when either agent captures its opponent’s flag or the blue agent is killed. The  $10 \times 10$  state space is fully observable, and there are 5 discrete actions for an agent: stay, up, right, down, and left. We aim to explain the policy used by the blue agent. The red agent uses a heuristic policy focused on defending its territory border (highlighted

---

### Algorithm 1 TL Greedy Search

---

**Input:** predicates  $\Psi := \{\psi_i\}$ , number of starts  $N_{\text{start}}$ , number of maximum search steps  $N_{\text{max}}$ , number of replicates  $N_{\text{rep}}$ , number of sampled states  $N_{\text{st}}$ , number of sampled episodes  $N_{\text{ep}}$ , target policy  $\pi_{\text{tar}}$ , reward filter threshold  $\tilde{R}_{\text{fin}}$   
**Output:** LTL explanation  $\phi$

- 1: Construct empty buffer  $\Phi$  to store output specification of each trace
- 2: Construct empty buffer  $U$  to store wKL divergence value of each output specification
- 3: **for**  $n = 1, 2, \dots, N_{\text{search}}$  **do**
- 4:   Initialize starting specification  $\tilde{\phi}$  randomly from  $\Psi$
- 5:   **for**  $m = 1, 2, \dots, N_{\text{max}}$  **do**
- 6:      $B = \text{SearchNeighbors}(\tilde{\phi}, \Psi, N_{\text{rep}}, N_{\text{st}}, N_{\text{ep}}, \pi_{\text{tar}}, \tilde{R}_{\text{fin}})$
- 7:      $\tilde{\phi}_{\text{max},1}, \tilde{U}_{\text{max},1} = B[0]$
- 8:     **if**  $\tilde{\phi} = \tilde{\phi}_{\text{max},1}$  **then**
- 9:       **for**  $i = 1, 2, \dots, N_{\text{extend}}$  **do**
- 10:          $\tilde{\phi}', \tilde{U}' \leftarrow B[i]$
- 11:          $B' = \text{SearchNeighbors}(\tilde{\phi}', \Psi, N_{\text{rep}}, N_{\text{st}}, N_{\text{ep}}, \pi_{\text{tar}}, \tilde{R}_{\text{fin}})$
- 12:          $\tilde{\phi}'_{\text{max},1}, \tilde{U}'_{\text{max},1} \leftarrow B'[0]$
- 13:         **if**  $\tilde{U}'_{\text{max},1} > \tilde{U}_{\text{max},1}$  **then**
- 14:            $\tilde{\phi}, \tilde{U} \leftarrow \tilde{\phi}'_{\text{max},1}, \tilde{U}'_{\text{max},1}$
- 15:           Go to line 6 and continue the search
- 16:         **else if**  $i = N_{\text{extend}}$  **then**
- 17:           Store  $\tilde{\phi}, \tilde{U}$  to  $\Phi, U$ , respectively
- 18:         **break**
- 19:         **else continue**
- 20:         **else**  $\tilde{\phi}, \tilde{U} \leftarrow \tilde{\phi}_{\text{max},1}, \tilde{U}_{\text{max},1}$
- 21:   Choose the best specification  $\phi$  from  $\Phi$  using  $\sigma$
- 22: **return**  $\phi$

---

in Figure 2). The agent will take the shortest path to the border region (if it is not already there) or randomly choose an action to stay in the border region (if it is already there). The agent takes a random action 25% of the time.

We defined four atomic predicates for this study, based on distances between objects in the environment. The general form for these predicates is  $\psi_{\text{Obj}_1, \text{Obj}_2} := d_{\text{Obj}_1, \text{Obj}_2} < c$ , where  $d_{\text{Obj}_1, \text{Obj}_2}$  is the euclidean distance between the objects and  $c$  is a constant. The four atomic predicates used were:  $\psi_{\text{RA}, \text{BF}} := d_{\text{RA}, \text{BF}} < 1.0$ ,  $\psi_{\text{BA}, \text{RF}} := d_{\text{BA}, \text{RF}} < 1.0$ ,  $\psi_{\text{BA}, \text{RA}} := d_{\text{BA}, \text{RA}} < 1.5$ ,  $\psi_{\text{BA}, \text{BT}} := d_{\text{BA}, \text{BT}} < 1.0$ , where BA, BF, BT, RA, and RF stand for the blue agent, blue flag, blue territory, red agent, and red flag, respectively. The resulting search space contains 640 specifications.

2) *Parking Environment*: We use the parking environment from [24], modified to include another vehicle that the ego vehicle must avoid when trying to reach the landmark parking spot. An episode terminates when the ego vehicle reaches the landmark, hits a wall, or hits the other vehicle. The state space is fully observable, and there are two continuous actions: steering angle  $\delta \in [-45^\circ, 45^\circ]$  and acceleration  $a \in [-5, 5]$  [m/s<sup>2</sup>]. We aim to explain the policy used by

---

**Algorithm 2** SearchNeighbors()

---

**Input:** starting specification  $\tilde{\phi}_{\text{in}}$ , predicates  $\Psi$ , number of replicates  $N_{\text{rep}}$ , number of sampled states  $N_{\text{st}}$ , number of sampled episodes  $N_{\text{ep}}$ , target policy  $\pi_{\text{tar}}$ , reward filter threshold  $\tilde{R}_{\text{fin}}$

**Output:** Buffer  $B$  of a neighbor LTL specification  $\tilde{\phi}_i$  and its KL divergence value  $\tilde{U}_{\tilde{\phi}_i}$  pairs sorted by the latter

- 1: Generate neighbor LTL specifications  $\tilde{\Phi}$  from  $\tilde{\phi}_{\text{in}}$  and  $\Psi$
  - 2: Construct a buffer  $B$  to store pairs of a KL divergence value and a neighbor specification
  - 3: **for**  $\tilde{\phi}_i$  in  $\tilde{\Phi}$  **do**
  - 4:   Synthesize automaton from  $\tilde{\phi}_i$
  - 5:   Optimize  $N_{\text{rep}}$  replicates  $\{\pi_{\text{rep}}\}$  for  $\tilde{\phi}_i$
  - 6:   Select a replicate  $\pi_{\tilde{\phi}_i}$  with the highest average non-trap state action distribution entropy
  - 7:   Calculate the node utility  $\tilde{U}_{\tilde{\phi}_i}$  using Equation (4).
  - 8:   Calculate the average converged reward  $r_{\text{fin}}$  from  $\pi_{\tilde{\phi}_i}$  for  $N_{\text{ep}}$  episodes.
  - 9:   **if**  $r_{\text{fin}} > \tilde{R}_{\text{fin}}$  **do**
  - 10:     Store  $(\tilde{U}_{\tilde{\phi}_i}, \tilde{\phi}_i)$  to  $B$
  - 11: **Sort**  $B$  in descending order by  $\tilde{U}_{\tilde{\phi}_i}$
  - 12:  $\tilde{\phi}_{\text{max}}, \tilde{U}_{\text{max}} = B[0]$
  - 13: **if**  $\tilde{\phi}_{\text{max}} = \tilde{\phi}_{\text{in}}$  **then**
  - 14:   Expand the neighborhood and repeat Lines 3-10
  - 15: **return**  $B$
- 

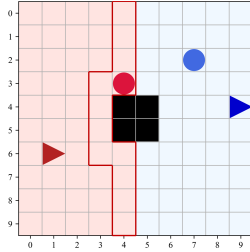


Fig. 2. Visualization of our 1 vs. 1 CtF game. Black squares are obstacles, triangles are flags, and circles are agents. The region highlighted by solid red lines is the border region for the red agent.

the ego vehicle. The ego vehicle is initialized at the center of the parking space  $(0, 0)$  with a random heading angle, with the other vehicle randomly initialized at one of four locations:  $(-30, 4)$ ,  $(30, 4)$ ,  $(30, -4)$ , and  $(-30, -4)$ . When initialized at  $(-30, 4)$  or  $(-30, -4)$ , the other vehicle heads to the right; it heads to the left when initialized at the other two locations. The steering angle of the other vehicle is fixed at  $0^\circ$ , with its acceleration  $a \in [-5, 5]$  [m/s<sup>2</sup>] being randomly selected at each time step. The maximum episode duration is 50 [s] and the policy control frequency is 5[Hz].

Similar to the CtF game, we defined three distance-based atomic predicates for this environment:  $\psi_{\text{ego,goal}} := d_{\text{ego,goal}} < 1$ ,  $\psi_{\text{ego,other}} := d_{\text{ego,other}} < 3$ ,  $\psi_{\text{ego,wall}} := d_{\text{ego,wall}} < 4$ , where ego and other stand for the ego and other

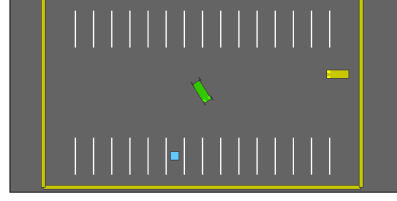


Fig. 3. Visualization of the parking environment. The green rectangle is the ego vehicle, the blue square is the landmark, and the yellow rectangle is the other vehicle. Yellow walls mark the boundary.

vehicles, respectively. The resulting search space contains 96 specifications.

### B. RL Training & Search Setup

We used the Stable Baselines3 [25] implementation of proximal policy optimization (PPO) [26] to optimize our target and searched policies for the CtF game, and soft actor critic (SAC) [27] with hindsight experience replay (HER) [28] for the parking environment. Our PPO implementation used a feed-forward neural network with two hidden layers (each containing 64 neurons) and a hyperbolic tangent activation function, and the following hyperparameters: learning rate of  $1 \times 10^{-5}$ , discount factor of 0.99, mini-batch size of 64, and 50,000 total time steps. Our SAC implementation used a feed-forward neural network with three hidden layers (each containing 512 neurons) and a hyperbolic tangent activation function, and the following hyperparameters: learning rate of  $1 \times 10^{-3}$ , buffer size of  $1 \times 10^6$ , discount factor of 0.99, batch size of 1024, and soft update coefficient of 0.05 with dense rewards. We used the following search hyperparameters:  $N_{\text{search}} = 10$  (number of independent searches),  $N_{\text{max}} = 10$  (number of maximum search steps),  $N_{\text{extend}} = 3$ ,  $N_{\text{st}} = 5,000$  (number of sampled states),  $N_{\text{ep}} = 200$  (number of sampled episodes), and  $\tilde{R}_{\text{fin}} = 0.05$ .

### C. CtF Results

We defined the target policy for the blue agent as an RL policy optimized for the LTL-specification  $\mathcal{F}(\psi_{\text{BA,RF}} \wedge \neg\psi_{\text{RA,BF}}) \wedge \mathcal{G}(\neg\psi_{\text{BA,RA}} \vee \psi_{\text{BA,BT}})$ . In plain English, this specification requires that: “Eventually, the blue agent reaches the red flag and does not reach the blue flag. Globally, the blue agent does not encounter the red agent or it stays in the blue territory.” We optimized three replicates for this specification and chose the one with the highest entropy, calculated using Equation (2).

Table II shows the resulting solutions found by our search algorithm over 10 random starts. We see that Searches 1 and 5 successfully found the true target specification as the specification with the highest utility (i.e., lowest wKL divergence) among searched specifications. Search 1 searched 8.13% of the search space while Search 5 searched 10.2% of it. The second best search result is Search 6, whose explanation is: “Eventually, the blue agent captures the red flag. Globally, the blue agent is not inside the blue territory while the red agent does not capture the blue flag, or the blue agent does

TABLE II

CTF EXPERIMENT SEARCH RESULTS. THE TARGET POLICY WAS SUCCESSFULLY FOUND IN SEARCHES 1 AND 5.

Search	LTL specification	wKL div. [-]	Searched specs [%]
1	$\mathcal{F}(\psi_{BA,RF} \wedge \neg\psi_{RA,BF}) \wedge \mathcal{G}(\neg\psi_{BA,RA} \vee \psi_{BA,BT})$	$8.00 \times 10^{-8}$	8.13
2	$\mathcal{F}((\neg\psi_{RA,BF}) \vee (\psi_{BA,RF})) \wedge \mathcal{G}(\neg\psi_{BA,RA} \vee \psi_{BA,BT})$	$5.95 \times 10^{-6}$	9.06
3	$\mathcal{F}((\neg\psi_{BA,RA}) \vee (\neg\psi_{RA,BF})) \wedge \mathcal{G}((\psi_{BA,BT}) \vee (\psi_{BA,RF}))$	$8.52 \times 10^{-5}$	6.56
4	$\mathcal{F}(\neg\psi_{BA,BT} \wedge \neg\psi_{RA,BF}) \wedge \mathcal{G}((\neg\psi_{BA,RF}) \vee (\neg\psi_{BA,RA}))$	$1.57 \times 10^{-6}$	6.56
5	$\mathcal{F}(\psi_{BA,RF} \wedge \neg\psi_{RA,BF}) \wedge \mathcal{G}(\neg\psi_{BA,RA} \vee \psi_{BA,BT})$	$8.00 \times 10^{-8}$	10.2
6	$\mathcal{F}(\psi_{BA,RF}) \wedge \mathcal{G}((\neg\psi_{BA,BT} \wedge \neg\psi_{RA,BF}) \vee (\neg\psi_{BA,RA}))$	$7.42 \times 10^{-7}$	8.44
7	$\mathcal{F}(\psi_{BA,RA}) \wedge \mathcal{G}((\neg\psi_{BA,BT}) \vee (\neg\psi_{BA,RF} \wedge \neg\psi_{RA,BF}))$	$1.18 \times 10^{-5}$	8.59
8	$\mathcal{F}(\neg\psi_{BA,RA}) \wedge \mathcal{G}((\neg\psi_{BA,RA} \wedge \psi_{BA,RF}) \vee (\neg\psi_{RA,BF}))$	$1.46 \times 10^{-8}$	6.56
9	$\mathcal{F}((\psi_{BA,RA}) \wedge (\neg\psi_{BA,RF})) \wedge \mathcal{G}((\psi_{BA,BT}) \vee (\neg\psi_{RA,BF}))$	$1.18 \times 10^{-5}$	11.4
10	$\mathcal{F}((\psi_{RA,BF}) \vee (\neg\psi_{BA,BT})) \wedge \mathcal{G}((\neg\psi_{BA,RA}) \vee (\psi_{BA,RF}))$	$1.62 \times 10^{-5}$	7.19

not encounter the red agent.” This explanation is close to the target LTL specification and consistent with the game dynamics. For example, the task (i.e.,  $\mathcal{F}(\bullet)$ ) part of the specification includes the overall objective of the blue agent capturing the red flag, while the constraint (i.e.,  $\mathcal{G}(\bullet)$ ) part plausibly captures the battle dynamics of our environment which could incentivize the blue agent to avoid the red agent if it is outside of the blue territory, but engage the red agent if both agents are in the blue territory. We also see that some searches did not find the target specification. This could be due to the fact that we are using LTL, which only truly considers deterministic environments, but considering stochastic environments (e.g. stochastic agent engagement in this CtF case).

We also implemented a random walk search to serve as a baseline comparison for our search method. We implemented this random walk by randomly initializing a starting specification, then randomly flipping a bit in that specification’s row vector representation until the target specification is reached. We performed this random walk 10,000 times and found that on average, a random walk reached the target specification after searching through 65.7% of the search space. For comparison, Searches 1 and 5 were approximately 6 times more efficient.

Figure 4 shows example RL training curves for two searched specifications. We see that the training curve for the solution specification from Search 1 converges to a positive return, meaning the optimized policy is able to satisfy the specification with some buffer. We also show a training curve for a “Nonsensical” specification that was searched, but unable to achieve a positive reward to motivate our implementation of the augmented return filter, as discussed in Section III-C. Close inspection of the actual specification shows that it is impossible to satisfy given the underlining game dynamics. More specifically, the specification requires  $\psi_{BA,RA} \wedge \psi_{BA,RF}$  to hold globally; this is impossible because the blue agent cannot be initialized on the red flag. It is also highly unlikely for the blue agent to stay next to the red agent for an entire episode.

Figure 5 shows a partial trace of the search tree produced by Search 5. We see that the extension step discussed in Section III-D was used in the third step of the search, which successfully kept the search from getting stuck in a sub-

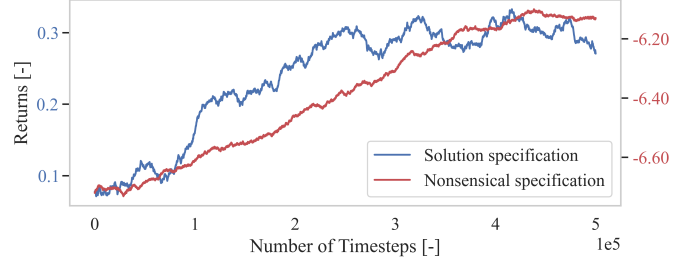


Fig. 4. Learning curves for the solution from Search 1,  $\mathcal{F}(\psi_{BA,RF} \wedge \neg\psi_{RA,BF}) \wedge \mathcal{G}(\neg\psi_{BA,RA} \vee \psi_{BA,BT})$ , and an example “Nonsensical” specification evaluated during the search process,  $\mathcal{F}(\neg\psi_{BA,BT} \wedge \neg\psi_{RA,BF}) \wedge \mathcal{G}(\psi_{BA,RA} \wedge \psi_{BA,RF})$ . Because nonsensical specifications have LTL reward functions that contradict the game dynamics, the converged return is below 0.

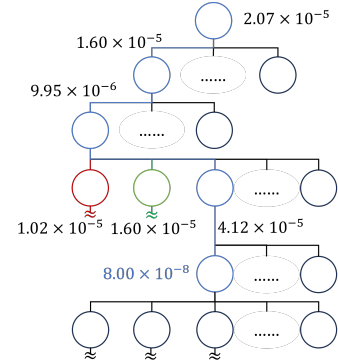


Fig. 5. A partial trace of Search 5 from Table II. Circles represent nodes with their corresponding wKL divergence values shown. The blue nodes and lines show how the local minimum moved as the search proceeded.

optimal local minimum early in the search process. More specifically, when the parent node in the third step was the local minimum (wKL divergence of  $9.95 \times 10^{-6}$ ) among its neighborhood after an expansion step, the red and green nodes’ neighborhoods were opened first and second, respectively, by the extension step. Subsequently, the neighborhood of the blue node next to the green node was opened and found a new local minimum whose wKL divergence value was  $8.00 \times 10^{-8}$ .

TABLE III

PARKING EXPERIMENT SEARCH RESULTS. THE TARGET POLICY WAS SUCCESSFULLY FOUND IN SEARCHES 1, 5, AND 7.

Search	LTL specification	wKL div. [-]	Searched specs [%]
1	$\mathcal{F}(\psi_{\text{ego,goal}}) \wedge \mathcal{G}(\neg\psi_{\text{ego,other}} \wedge \neg\psi_{\text{ego,wall}})$	<b>0.00</b>	37.5
2	$\mathcal{F}(\neg\psi_{\text{ego,other}} \wedge \psi_{\text{ego,wall}}) \wedge \mathcal{G}(\neg\psi_{\text{ego,goal}})$	$7.35 \times 10^{-4}$	28.1
3	$\mathcal{F}(\neg\psi_{\text{ego,other}} \wedge \psi_{\text{ego,wall}}) \wedge \mathcal{G}(\neg\psi_{\text{ego,goal}})$	$7.35 \times 10^{-4}$	27.1
4	$\mathcal{F}(\psi_{\text{ego,wall}}) \wedge \mathcal{G}(\neg\psi_{\text{ego,goal}} \vee \psi_{\text{ego,other}})$	$6.40 \times 10^{-4}$	30.2
5	$\mathcal{F}(\psi_{\text{ego,goal}}) \wedge \mathcal{G}(\neg\psi_{\text{ego,other}} \wedge \neg\psi_{\text{ego,wall}})$	<b>0.00</b>	29.2
6	$\mathcal{F}(\psi_{\text{ego,other}}) \wedge \mathcal{G}(\neg\psi_{\text{ego,goal}} \vee \neg\psi_{\text{ego,wall}})$	$4.61 \times 10^{-4}$	44.8
7	$\mathcal{F}(\psi_{\text{ego,goal}}) \wedge \mathcal{G}(\neg\psi_{\text{ego,other}} \wedge \neg\psi_{\text{ego,wall}})$	<b>0.00</b>	37.5
8	$\mathcal{F}(\psi_{\text{ego,other}}) \wedge \mathcal{G}(\neg\psi_{\text{ego,goal}} \vee \neg\psi_{\text{ego,wall}})$	$4.61 \times 10^{-4}$	33.3

#### D. Parking Experiment

We defined the target policy of the ego vehicle as an RL policy optimized for specification  $\mathcal{F}(\psi_{\text{ego,goal}}) \wedge \mathcal{G}(\neg\psi_{\text{ego,other}} \wedge \neg\psi_{\text{ego,wall}})$ , which requires that: “*Eventually, the ego vehicle reaches the goal. Globally, the ego vehicle does not hit the other vehicle and walls.*” We again optimized two replicates and chose the one with the highest entropy.

Table III shows the specifications found by our search algorithm over eight random starts. Searches 1, 5, and 7 successfully found the true target specification, with each searching 37.5%, 29.2%, and 33.3% of the search space, respectively. The second best results were Searches 6 and 8, which found the same solution whose explanation is: “*Eventually, the ego vehicle encounters the other agent. Globally, the ego vehicle does not reach the goal or does not hit the wall.*” This explanation captures a failure case, where the ego vehicle sometimes does not reach the goal because it collides with the other vehicle, though it does successfully avoid walls. This result suggests that the resulting explanation from a search can capture unlikely, but observed, behaviors from the target policy that occur due to the stochastic nature of the environment.

Furthermore, we see that each search optimized and evaluated less than 45% of the specifications in the entire search space. As in Section IV-C, we implemented a baseline random walk search, which on average searched through 66.5% of the search space. In comparison, Searches 1, 5, and 7 were about twice as efficient.

#### V. CONCLUSIONS

This paper introduces a method for generating explanations for *reinforcement learning* (RL) policies using a connected family of *linear temporal logic* (LTL) formulae. It is possible to transform any member of this family to another by a series of unitary syntax modifications that form the basis of a local-search described in the paper. Reference [9] outlines an approach for converting an LTL-specification into an equivalent policy. In our work, we tackle the reverse problem: identifying the optimal LTL-explanation for a given target policy. We achieve this through a local-search algorithm with multiple starting points applied to the family of LTL-formulae, resulting in an associated policy that minimizes the weighted *Kullback-Leibler* (KL) divergence from the target policy. To validate our approach, we generated target policies using user-defined LTL-specifications for

two robotics applications, and show that our proposed search procedure successfully identifies each target specification.

Many future research avenues exist to expand our method or address its current limitations. First, our approach requires one to articulate the set of atomic predicates used within potential explanation specifications. Selecting inappropriate ones can yield unreliable explanations, while selecting many irrelevant ones can yield infeasible computational requirements. Establishing guidelines, or an automated procedure, for the selection of atomic predicates would greatly improve the generalization and scalability of our method (and many other related ones in the field of mining temporal logic specifications). Our proposed method also requires one to optimize an RL policy for each searched node. Implementing transfer learning techniques, such as warm-starting optimization from pretrained similar policies, could reduce overall required training time. Future directions also include exploring alternatives to LTL that better capture environment stochasticity or partial observability, alternative metrics for evaluating policy similarity, alternative neighborhood definitions, and alternative specification templates. Finally, another interesting direction is to explore ways to integrate foundational large language models with formal methods (like LTL) for generating explanations that preserve mathematical preciseness (e.g., building from [29]). The procedure outlined in this paper can serve as a foundational framework for exploring such future work.

#### REFERENCES

- [1] D. Silver, T. Hubert, J. Schrittwieser, I. Antonoglou, M. Lai, A. Guez, M. Lanctot, L. Sifre, D. Kumaran, T. Graepel, T. Lillicrap, K. Simonyan, and D. Hassabis, “A general reinforcement learning algorithm that masters chess, shogi, and Go through self-play,” *Science*, vol. 362, pp. 1140–1144, Dec. 2018. Publisher: American Association for the Advancement of Science.
- [2] S. Zhang, L. Yao, A. Sun, and Y. Tay, “Deep Learning Based Recommender System: A Survey and New Perspectives,” *ACM Computing Surveys*, vol. 52, pp. 5:1–5:38, Feb. 2019.
- [3] H. Nguyen and H. La, “Review of Deep Reinforcement Learning for Robot Manipulation,” in *2019 Third IEEE International Conference on Robotic Computing (IRC)*, pp. 590–595, Feb. 2019.
- [4] D. Silver, J. Schrittwieser, K. Simonyan, I. Antonoglou, A. Huang, A. Guez, T. Hubert, L. Baker, M. Lai, A. Bolton, Y. Chen, T. Lillicrap, F. Hui, L. Sifre, G. van den Driessche, T. Graepel, and D. Hassabis, “Mastering the game of Go without human knowledge,” *Nature*, vol. 550, pp. 354–359, Oct. 2017. Number: 7676 Publisher: Nature Publishing Group.
- [5] K. Arulkumaran, M. P. Deisenroth, M. Brundage, and A. A. Bharath, “Deep Reinforcement Learning: A Brief Survey,” *IEEE Signal Processing Magazine*, vol. 34, pp. 26–38, Jan. 2017. Conference Name: IEEE Signal Processing Magazine.

- [6] J. Chen, S. E. Li, and M. Tomizuka, "Interpretable End-to-End Urban Autonomous Driving With Latent Deep Reinforcement Learning," *IEEE Transactions on Intelligent Transportation Systems*, vol. 23, pp. 5068–5078, June 2022. Conference Name: IEEE Transactions on Intelligent Transportation Systems.
- [7] A. Heuillet, F. Couthouis, and N. Díaz-Rodríguez, "Explainability in deep reinforcement learning," *Knowledge-Based Systems*, vol. 214, p. 106685, Feb. 2021.
- [8] E. Bartocci, C. Mateis, E. Nesterini, and D. Nickovic, "Survey on mining signal temporal logic specifications," *Information and Computation*, vol. 289, p. 104957, Nov. 2022.
- [9] X. Li, Z. Serlin, G. Yang, and C. Belta, "A formal methods approach to interpretable reinforcement learning for robotic planning," *Science Robotics*, vol. 4, p. eaay6276, Dec. 2019. Publisher: American Association for the Advancement of Science.
- [10] R. Yan, A. Julius, M. Chang, A. Fokoue, T. Ma, and R. Uceda-Sosa, "STONE: Signal Temporal Logic Neural Network for Time Series Classification," in *2021 International Conference on Data Mining Workshops (ICDMW)*, pp. 778–787, Dec. 2021. ISSN: 2375-9259.
- [11] N. Baharisangari, K. Hirota, R. Yan, A. Julius, and Z. Xu, "Weighted Graph-Based Signal Temporal Logic Inference Using Neural Networks," *IEEE Control Systems Letters*, vol. 6, pp. 2096–2101, 2022.
- [12] Z. Xu, M. Ornik, A. A. Julius, and U. Topcu, "Information-Guided Temporal Logic Inference with Prior Knowledge," in *2019 American Control Conference (ACC)*, pp. 1891–1897, July 2019. ISSN: 2378-5861.
- [13] G. Bombara and C. Belta, "Offline and Online Learning of Signal Temporal Logic Formulae Using Decision Trees," *ACM Transactions on Cyber-Physical Systems*, vol. 5, pp. 22:1–22:23, Mar. 2021.
- [14] S. Arora and P. Doshi, "A survey of inverse reinforcement learning: Challenges, methods and progress," *Artificial Intelligence*, vol. 297, p. 103500, Aug. 2021.
- [15] R. S. Sutton, D. Precup, and S. Singh, "Between MDPs and semi-MDPs: A framework for temporal abstraction in reinforcement learning," *Artificial Intelligence*, vol. 112, pp. 181–211, Aug. 1999.
- [16] M. L. Littman, "Markov games as a framework for multi-agent reinforcement learning," in *Machine Learning Proceedings 1994* (W. W. Cohen and H. Hirsh, eds.), pp. 157–163, San Francisco (CA): Morgan Kaufmann, Jan. 1994.
- [17] G. Kahn, A. Villalbor, B. Ding, P. Abbeel, and S. Levine, "Self-Supervised Deep Reinforcement Learning with Generalized Computation Graphs for Robot Navigation," in *2018 IEEE International Conference on Robotics and Automation (ICRA)*, pp. 5129–5136, May 2018. ISSN: 2577-087X.
- [18] K. Schneider, "Improving Automata Generation for Linear Temporal Logic by Considering the Automaton Hierarchy," in *Logic for Programming, Artificial Intelligence, and Reasoning* (R. Nieuwenhuis and A. Voronkov, eds.), Lecture Notes in Computer Science, (Berlin, Heidelberg), pp. 39–54, Springer, 2001.
- [19] A. Duret-Lutz, E. Renault, M. Colange, F. Renkin, A. Gbaguidi Aisse, P. Schlehuter-Caissier, T. Medioni, A. Martin, J. Dubois, C. Gillard, and H. Lauko, "From Spot 2.0 to Spot 2.10: What's New?," in *Computer Aided Verification* (S. Shoham and Y. Vizel, eds.), vol. 13372, pp. 174–187, Cham: Springer International Publishing, 2022. Series Title: Lecture Notes in Computer Science.
- [20] R. Oura, A. Sakakibara, and T. Ushio, "Reinforcement Learning of Control Policy for Linear Temporal Logic Specifications Using Limit-Deterministic Generalized Büchi Automata," *IEEE Control Systems Letters*, vol. 4, pp. 761–766, July 2020. Conference Name: IEEE Control Systems Letters.
- [21] C. Sun, X. Li, and C. Belta, "Automata Guided Semi-Decentralized Multi-Agent Reinforcement Learning," in *2020 American Control Conference (ACC)*, pp. 3900–3905, July 2020. ISSN: 2378-5861.
- [22] X. Li, C.-I. Vasile, and C. Belta, "Reinforcement learning with temporal logic rewards," in *2017 IEEE/RSJ International Conference on Intelligent Robots and Systems (IROS)*, pp. 3834–3839, Sept. 2017. ISSN: 2153-0866.
- [23] B. D. Ziebart, A. L. Maas, J. A. Bagnell, A. K. Dey, *et al.*, "Maximum entropy inverse reinforcement learning," in *AAAI*, vol. 8, pp. 1433–1438, Chicago, IL, USA, 2008.
- [24] E. Leurent, "An environment for autonomous driving decision-making." <https://github.com/eleurent/highway-env>, 2018.
- [25] A. Raffin, A. Hill, A. Gleave, A. Kanervisto, M. Ernestus, and N. Dormann, "Stable-baselines3: Reliable reinforcement learning implementations," *Journal of Machine Learning Research*, vol. 22, no. 268, pp. 1–8, 2021.
- [26] J. Schulman, F. Wolski, P. Dhariwal, A. Radford, and O. Klimov, "Proximal Policy Optimization Algorithms," Aug. 2017. arXiv:1707.06347 [cs].
- [27] T. Haarnoja, A. Zhou, P. Abbeel, and S. Levine, "Soft Actor-Critic: Off-Policy Maximum Entropy Deep Reinforcement Learning with a Stochastic Actor," Aug. 2018. arXiv:1801.01290 [cs, stat].
- [28] M. Andrychowicz, F. Wolski, A. Ray, J. Schneider, R. Fong, P. Welinder, B. McGrew, J. Tobin, P. Abbeel, and W. Zaremba, "Hindsight Experience Replay," Feb. 2018. arXiv:1707.01495 [cs].
- [29] Y. Chen, R. Gandhi, Y. Zhang, and C. Fan, "NL2TL: Transforming Natural Languages to Temporal Logics using Large Language Models," in *Proceedings of the 2023 Conference on Empirical Methods in Natural Language Processing* (H. Bouamor, J. Pino, and K. Bali, eds.), (Singapore), pp. 15880–15903, Association for Computational Linguistics, Feb. 2023.